

Letters

Kinetics of craze propagation in polymethylmethacrylate and polycarbonate in n-butyl alcohol

Polymethylmethacrylate and polycarbonate are finding many uses as industrial materials, such as in automobiles and other consumer goods. Of particular interest to the manufacturer and consumer alike, is their resistance to mechanical degradation under stress in certain unfavourable environments, such as organic solvents. Under certain conditions, these materials are subject to the phenomenon of crazing. This phenomenon [1] grows by meniscus instability, as proposed by Argon, and not by cavitation as was previously thought. The formation of crazes is the precursor to cracking and subsequent failure of the materials under stress. In the present work, the effects of stress and temperature on the kinetics of crazing in an environment of *n*-butyl alcohol are studied.

Marshall, Culver and Williams [2] studied craze propagation in single-edge notched specimens of polymethylmethacrylate under tension in a methylalcohol environment.

Using a simplified form of the Navier–Stokes equation for convective flow in channels, they developed theoretical equations for craze length, x , as a function of time, t , for the case of a rate limiting flow through the sides of the specimens, normal to the direction of craze growth.

For the end flow condition,

$$x = \left(\frac{l_0 \bar{P}}{10\sigma_y E \eta} \right)^{\frac{1}{2}} (K_0 - K_m) t^{\frac{1}{2}}, \quad (1)$$

where l_0 is the average distance between sites of dishomogeneity in the plastic zone, K_0 is the stress intensity factor calculated using the initial length of the crack, K_m is a lower limiting value of K_0 , σ_y is the yield strength of the material at the crack tip, E is the modulus of elasticity, \bar{P} is the pressure of the environment at the edge of the notched specimen and η is the viscosity of the solvent at the temperature of the test.

For side-flow conditions, the craze length, x , is proportional to time

$$x = \frac{1}{2} \Delta H \left(\frac{l_0 \bar{P}}{10\sigma_y E \eta} \right)$$

$$\times [(K_0 - K_m)^2 - (K_n - K_m)^2] t, \quad (2)$$

where Δ is a constant, H is the specimen thickness and K_n is an upper limiting value of K_0 .

It was found that below a certain value of the stress intensity factor, $K_0 = K_m$, there was no visible craze propagation while for values of stress intensity factor between K_m and a higher limiting value of K_n , the rate of craze propagation was described by the end-flow model. For values of K_0 greater than K_n , up to the critical stress intensity factor, the craze length increased with a power of time between $\frac{1}{2}$ and 1, indicating that a combination of end-flow and side-flow controlled the rate of growth. In later work, Marshall also reported the effect of temperature on the above mentioned parameters [3].

In a more recent study, Kramer and Bubeck [4] hypothesized a model similar to that of Marshall *et al.*, but using the driving force of capillary action to characterize the flow of solvent through the craze. The Kramer–Bubeck model reduces to the same form as the Marshall model in particular cases of end-flow, but can take on powers of time both greater and less than $\frac{1}{2}$ in other cases. Their results are in accord with the prior results reported in the literature.

The materials chosen for study were polymethylmethacrylate (PMMA, from Vedril Montedison) and polycarbonate (PC, from Lexan General Electric). Compact tensile specimens, of geometry specified by ASTM Standard Number E 339-74 (see Fig. 1) were machined from extruded sheets of dimensions 1 m × 3 m × 12 mm.

A mechanically operated wedge, was used to propagate a natural crack from the machined notch. The length of the natural crack could be precisely controlled by putting a light compression at the end of the desired growth zone, perpendicular to the direction of growth. The compression was transmitted through two metal blocks positioned appropriately on the edges of the specimen. The cracks obtained at room temperature in PMMA closely resembled those obtained in fatigue. The crack surfaces appeared silvery and flat and the leading edge of the crack was nearly rectilinear. Furthermore, the rate of pro-

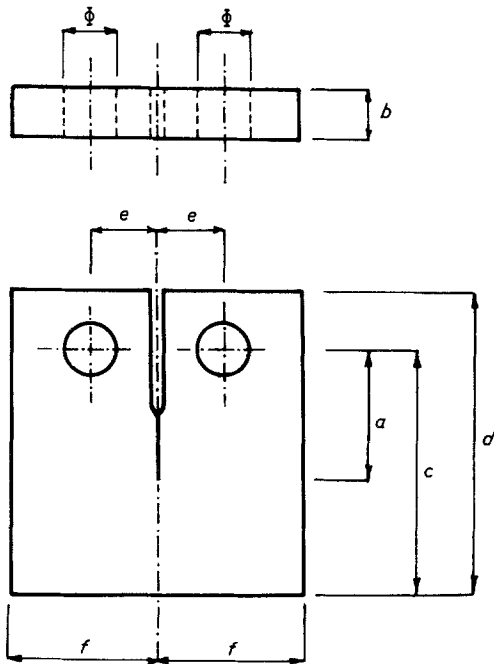


Figure 1 Dimensions and configuration of the compact tensile specimens, according to [5] where w is the specimen width, $c = w \pm 0.005w$, $d = 1.25w \pm 0.010w$, $e = 0.275w \pm 0.005w$, $f = 0.6w \pm 0.005w$ and $\Phi = 0.25w \pm 0.005w$.

propagation of the crack produced by the wedge was easily controllable.

The technique had to be modified for application to polycarbonate. Natural cracks in PC specimens have been successfully obtained by the same method but with the specimens and the operated wedge held at a temperature of 80 K, in liquid nitrogen.

All craze propagation measurements were carried out at constant temperature and load while the specimen was immersed in *n*-butyl alcohol. Since the materials were transparent, the propagation could be observed optically. A two-litre glass tank was used to contain the alcohol. The top was open and the bottom possessed a gasketed hole to accept a stationary connecting rod from an Instron 1112 testing machine. The vessel was fixed to the lower grip and rod through the gasketed hole and the sample was fixed between the two grips by loading pins. The upper grip and rod were connecting directly to the load cell of the Instron machine.

Upon one surface of the specimen a grid of uniform lines was scratched so as to measure the

rate of craze propagation directly. The specimen was back-lit to highlight the craze and the craze growth was observed using a cathetometer.

The rate of craze growth was correlated to the stress intensity factor K , using the same method as that used in [5].

Polymethylmethacrylate. The kinetics of craze propagation were studied at 8°C, 15°C and 35°C. Typical data of craze length against time at a constant value of stress intensity factor K_0 are shown in Fig. 2, plotted in logarithmic co-ordinates. A straight line with a slope of 0.5 indicates a dependence of craze length on the square root of time in accordance with the end-flow model of Marshall (Equation 1). Equation 1 may be re-written in the form

$$x/t^{1/2} = m(T)K_0 - m(T)K_m, \quad (4)$$

where

$$m(T) = \left(\frac{I_0 \bar{P}}{10\sigma_y E \eta} \right)^{1/2} \quad (5)$$

is a measure of the rate constant and K_m is the lower limiting value of the stress intensity factor, below which craze propagation does not occur. The quantity $m(T)$ should be temperature dependent, primarily because of the temperature dependence of the fluid viscosity, $\eta(T)$.

Fig. 3 is a plot of the data for various values of K_0 and temperature. Each mean value of $x/t^{1/2}$ was obtained from linear regression analysis of the raw data. A linear increase in $x/t^{1/2}$ can be seen, with the slope increasing with temperature, until a maximum value is attained in the vicinity of $K_0 = 35 \text{ N mm}^{-3/2}$. Thereafter, the value of

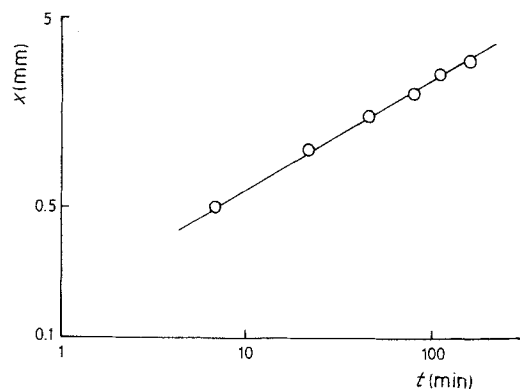


Figure 2 Typical data of craze length, x , plotted against time, t , at a constant value of stress intensity factor for PMMA.

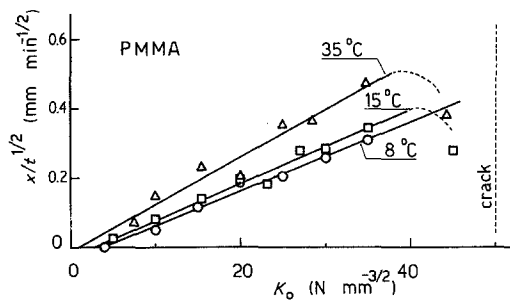


Figure 3 ($x/t^{1/2}$) data plotted against K_0 at different temperatures as indicated, for PMMA.

$x/t^{1/2}$ tends to decrease. At a value of $K_0 = 50 \text{ N mm}^{-3/2}$ the material breaks spontaneously, signifying that the material is near the critical stress intensity factor, K_{0c} . The critical stress intensity factor, K_{0c} , appears to be relatively independent of temperature.

In order to estimate values for $m(T)$ and K_m as a function of temperature, the values of $x/t^{1/2}$ below K_0 at the maxima (i.e. $35 \text{ N mm}^{-3/2}$) were fit to a straight line using linear regression analysis. The results together with the correlation coefficient, r^2 , are tabulated in Table I for the three temperatures. The value of $m(T)$ increases monotonically with temperature, while K_m decreases by 73% over the temperature range 8°C to 35°C .

From Equation 5, it can be seen that the slope $m(T)$ is related to the properties of the polymer and solvent. The ratio $(l_0 \bar{P} / \sigma_y E)$ should be more or less independent of temperature over the range studied and, accordingly, the ratios of the slopes $m(T)$ at the two temperatures should be approximately equal to the inverse ratio of the square roots of the viscosities of the *n*-butyl alcohol, $\eta(T)$. This, in fact, is the case:

$$\frac{m(8)}{m(15)} = 0.95; \left(\frac{\eta(15)}{\eta(8)} \right)^{1/2} = 0.92$$

and

$$\frac{m(8)}{m(35)} = 0.73; \left(\frac{\eta(35)}{\eta(8)} \right)^{1/2} = 0.73.$$

TABLE I Values of $m(T)$, K_m and r^2 (see text) at different temperatures for PMMA in *n*-butyl alcohol

$T(^{\circ}\text{C})$	$m(T) (\times 10^2)$	$K_m (\text{N mm}^{-3/2})$	r^2
8	1.000	3.82	0.99
15	1.056	2.66	0.98
35	1.376	1.04	0.95

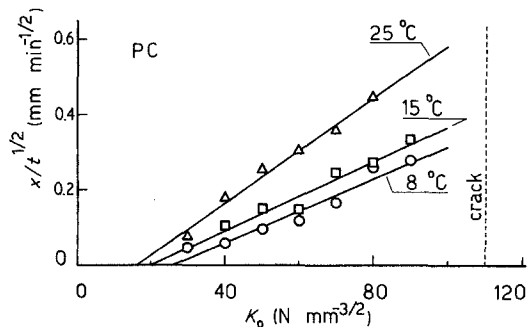


Figure 4 ($x/t^{1/2}$) data plotted against K_0 at different temperatures as indicated, for PC.

Thus it appears that, at least for stress intensity factors less than about $35 \text{ N mm}^{-3/2}$ (about 66% of the critical stress intensity), convective flow of solvent through the end of the craze controls the rate of craze propagation in polymethylmethacrylate. Using the physical model of Marshall, it may be hypothesized that, at stress intensity values greater than $35 \text{ N mm}^{-3/2}$, the stress causes lateral contraction of the free surfaces, minimizing the plane-strain deformation and suppressing the formation of microvoids. This could lead to a decrease of convection flow of solvent and a slowing down of the growing craze, thus accounting for the decrease in the value of $x/t^{1/2}$.

Polycarbonate. The kinetics of craze propagation of polycarbonate in *n*-butyl alcohol was studied at 8°C , 15°C and 25°C .

As with polymethylmethacrylate, the craze length varied with the square root of time for every temperature and value of K_0 studied. Values of $x/t^{1/2}$ at each condition were calculated, as described previously for the PMMA data, and were plotted as a function of K_0 at the three temperatures. The results are shown in Fig. 4 and the general trends are similar to those obtained for the PMMA. Linear regression analysis was used to correlate the data to a straight line. The values of $m(T)$, K_m and the correlation coefficient, r^2 , from a best-fit of the data are shown in Table II. Even in

TABLE II Values of $m(T)$, K_m and r^2 (see text) at different temperatures for PC in *n*-butyl alcohol

$T(^{\circ}\text{C})$	$m(T) (\times 10^2)$	$K_m (\text{N mm}^{-3/2})$	r^2
8	0.423	25.4	0.94
15	0.463	19.8	0.96
25	0.699	16.1	0.99

this case it appears that both the slope, $m(T)$, and the minimum value of the stress intensity factor, K_m , vary monotonically with temperature. The ratios of slopes at different temperatures may be compared to the inverse ratios of the square roots of viscosities:

$$\frac{m(8)}{m(25)} = 0.61; \quad \left(\frac{\eta(25)}{\eta(8)} \right)^{\frac{1}{2}} = 0.80$$

and

$$\frac{m(15)}{m(25)} = 0.66; \quad \left(\frac{\eta(25)}{\eta(15)} \right)^{\frac{1}{2}} = 0.82.$$

Unlike for the PMMA results, no close agreement is seen, indicating that the temperature dependences of the other factors in $m(T)$ (i.e. of l_0 , \bar{P} , σ_y and E) may be important also. There is not enough information to separate the various factors, but it is likely that the local yielding properties and the density of microvoid formation are more sensitive to temperature than was the case for the PMMA. The minimum stress intensity factor, K_m , decreases by 37% over the temperature range 8°C to 25°C, indicating that craze initiation is easier (i.e. requires less stress) at the higher temperature.

Acknowledgement

The authors wish to express their gratitude to the National Science Foundation (USA) for providing

financial support to ATD under the Science Faculty Professional Development Program.

References

1. A. M. DONALD and E. J. KRAMER, Report number 4233, Materials Science Center, Cornell University, USA, 1979.
2. G. P. MARSHALL, L. E. CULVER and J. G. WILLIAMS, Proc. Roy. Soc. A-319 (1970) 165.
3. J. G. WILLIAMS and G. P. MARSHALL, in "Deformation and Fracture of High Polymers: Battelle Institute, Material Science Colloquia" Vol. 7, edited by H. H. Kausch, J. A. Hassel and R. J. Jaffee (Plenum Press, New York, 1973) p. 557.
4. E. J. KRAMER and R. A. BUBECK, *J. Polymer Sci., Polymer Plastic Edn.* 16 (1978) 1195.
5. ASTM Standard Number E 399-74 (1974).

Received 12 June
and accepted 30 October 1980.

A. T. DI BENEDETTO*
P. BELLUSCI
M. IANNONE
L. NICOLAIS

*Istituto di Principi di Ingegneria Chimica,
University of Naples,
80125 Naples,
Italy*

*On leave from: Department of Chemical Engineering and Institute of Materials Science, University of Connecticut Storrs, Connecticut, USA.

Crystallographic relationships arising during the cellular growth of the Cd-Zn eutectic

This work is part of the general study of eutectics which has been in progress in the authors' laboratory for some time. Earlier studies were principally concerned with the development of a characterisation scheme for eutectic morphologies [1-3]. This was followed by a detailed analysis of the mechanical properties of various members of the characteristic morphological groups [4-8]. In one system in particular, Cd-Zn [9], tested in both tension and compression, it was found that the strength of the eutectic composite increased significantly as the specimen growth rate, R , was

increased: the ultimate tensile strength (UTS) increased from 107 to 186 N mm⁻² and the ultimate compressive strength (UCS) increased from 176 to 420 N mm⁻². However, the increase in R was accompanied by a decrease in lamellar spacing, λ , and an increase in cellular growth, shown in Fig. 1a, which was found to be particularly pronounced at a growth rate, R , of 4000 mm h⁻¹, the fastest speed used. As a result, it was not clear whether cellular growth, or both of these changes, was responsible for the increased strength.

In the Cd-Zn eutectic, both phases have a close-packed hexagonal structure and grow with $(0001)_{\text{Cd}} \parallel (0001)_{\text{Zn}}$ and $[01\bar{1}0]_{\text{Cd}} \parallel [01\bar{1}0]_{\text{Zn}}$ [10, 11]. The unit cell dimension c/a ratios for